Relating Skewness and Fourier Harmonics in Low Reynolds Number Wake Flow

Krithsanvith Manthripragada*, Theresa Saxton-Fox†
University of Illinois at Urbana-Champaign, Urbana, Illinois 61801.

Simple, laminar wake flows require many Fourier modes to represent their dynamics, even though they are perfectly periodic with a single period. The spatial form of the Fourier modes alternate between having a maximum value in the center of the wake for odd harmonics and having a zero crossing in the center of the wake for even harmonics of the primary frequency. We demonstrate that the harmonic organization and the alternating shapes of the vorticity Fourier modes for simple wakes are direct results of the skewness of the wake's vorticity field. Through analysis of simple mathematical models and investigation of laminar wake data, we show that having a non-zero skewness guarantees that more than one Fourier mode is required to represent the dynamics, even for a perfectly periodic signal. We also define the mathematical relationship between the skewness of data and the phase of the Fourier modes that can represent that data, and connect those phase relationships to the spatial structure of the Fourier modes.

I. Nomenclature

ϕ	=	Skewness
s	=	Example signal
θ	=	Vector of parameters
t	=	Time
ω	=	Vorticity
x	=	Streamwise coordinate
y	=	Vertical coordinate
ρ	=	Density
U	=	Free stream velocity
L	=	Chord length
μ	=	Viscosity
f^*	=	Normalized frequency
ω_0	=	Fundamental angular frequency
α_r	=	Amplitude of r-th harmonic
γ_r	=	Phase of r-th harmonic
A_M	=	Amplitude modulation coefficient
Re	=	Reynolds number

II. Introduction

The Fourier transform is a key tool in fluid flow analysis, providing insights into the critical frequencies present in the flow field and into the spatial structure of the flow at those frequencies. Sirovich and Knight [1] and Foias et al. [2] applied the Fourier transform to identify the spectral properties of turbulent flows, shedding light on the asymptotic behavior of eigenfunctions in higher dimensions. Often, harmonic Fourier modes are observed in Fourier transforms of fluid dynamic signals. Harmonics are multiples of a core fundamental frequency. Having energetic harmonics in a signal does not not necessarily reflect that a problem has multiple dynamic time scales in the sense of a multi-scale turbulent flows. Laminar problems with no multi-scale dynamics frequently exhibit harmonic Fourier modes.

*Graduate Research Assistant, Mechanical Science and Engineering, 1308 W Green St, Urbana, Illinois 61801.
†Assistant Professor, Aerospace Engineering, 104 S Wright St, Urbana, Illinois 61801, AIAA Member.

The harmonics that appear in Fourier transforms of a data set are mathematically related to the skewness of that data [3]. Skewness is a measure of asymmetry in probability distributions. A symmetric Gaussian distribution has zero skewness, but a signal that has extreme, strong events larger (smaller) than its mean and frequent but weak events smaller (larger) than its mean will have positive (negative) skewness. Many flows in fluid dynamics have non-zero skewness. The skewness, ϕ, of a given signal, $s(t)$, is expressed mathematically as the third central moment divided by the cube of the standard deviation of the signal,

$$\phi_{(s(\theta,t))} = \frac{E\{s^3(\theta,t)\}}{(E\{s^2(\theta,t)\})^{3/2}}. \tag{1}$$

Here, θ indicates other parameters that a signal s may depend on besides time, and E is the expectation operator. The importance of skewness in turbulent wall-bounded flows has been previously explored in the context of amplitude modulation and triadic interactions between dynamically distinct flow features. The amplitude modulation coefficient, R, is directly mathematically related to the skewness, ϕ, of a signal [4, 5]. The amplitude modulation coefficient quantifies whether small scales are more or less amplified during positive versus negative large-scale fluctuations. If small-scale fluctuations are stronger when large scales are positive (negative), then the positive (negative) extrema in the signal are stronger than the negative (positive) extrema, giving positive (negative) skewness. Duvvuri and McKeon [6] extend the understanding by investigating all triadic scale interactions in turbulent boundary layers and relating those interactions to skewness.

Much of the research which explores the relationship between skewness and Fourier modes in turbulent flows has focused on wall-bounded turbulent flows, which exhibit negligible large-scale skewness, as seen in the works of Schlatter and Örlü [4], Marusic et al. [5], and Duvvuri and McKeon [6]. For those flows, the interaction between dynamically distinct modes is the largest contributor to the skewness for the majority of the spatial field. The motivation of this paper is to understand the relationship between skewness and Fourier modes in flows characterized by high large-scale skewness, such as wake flows like flat plate vortex shedding. The implications of this relationship include a deeper understanding of the physical meaning of Fourier modes, an improved ability to predict the shape of Fourier modes apriori, and an improved ability to distinguish Fourier modes that reflect features of large-scale structures versus genuinely distinct small-scale dynamics. We focus on a laminar flow that has no multi-scale dynamics but does exhibit harmonic Fourier modes to better highlight the relationship between skewness and harmonic Fourier modes.

III. Simple wake flow

In this work, we choose to focus on the relationship between harmonics and skewness in a flow that has significant large-scale skewness and that has no small-scale dynamics that could yield amplitude modulation or triadic interactions outside of harmonic relationships. This choice allows us to understand the impact on skewness on the Fourier transform's representation of the large-scale dynamics, and will be used as a first step towards ultimately understanding more complex, multi-scale, skewed flows. We use low Reynolds number flat plate vortex shedding data based on the immersed-boundary method, as outlined by Goza and Colonius (2017) [7]. The flat plate was positioned at a 35° angle of attack, with a Reynolds number Re of 100. The spatial grid and time-step dimensions were maintained at $\Delta x = 0.04$ and $\Delta t = 0.001$ respectively. The simulation was executed for a sufficient duration to ensure the attainment of limit-cycle dynamics. The flat plate, operating at a stall angle of attack, induced periodic shedding of vortices at the leading and trailing edges, as visually depicted in the instantaneous snapshots presented in Figure 1.

Figure 1 displays four instantaneous snapshots capturing the vorticity field, offering a visual portrayal of the vortex shedding phenomenon occurring distinctly at the leading and trailing edges of the flat plate. This is a perfectly periodic flow field and has only one dynamic scale. To analyze the flow dynamics around the flat plate, we employed the Fast Fourier Transform (FFT) methodology on the vorticity data.

Figure 2 illustrates the spectral density plot obtained from the FFT analysis. This plot reveals the energy distribution across various frequencies, with sharp peaks indicating the dominant frequencies that characterize the flow's dynamic behavior. The largest peak, at 0.7 frequency represents the frequency of vortex shedding. The three next largest peaks are at 1.4, 2.1, 2.8 frequencies. These are exactly twice, three times, and four times the vortex shedding frequency. These peaks indicate the presence of harmonics in the Fourier modes. The frequencies are normalized by the chord length L and freestream velocity U, expressed as $f^* = \frac{L}{\Delta t \cdot U}$.

The four Fourier modes of the vorticity field with the largest amplitude in the power spectrum are shown in figure 3. From left to right, they correspond to the temporal frequencies of 0.7, 1.4, 2.1, 2.8, such that the first represents the fundamental vortex shedding frequency, the second its second harmonic, the third a frequency of three times the vortex

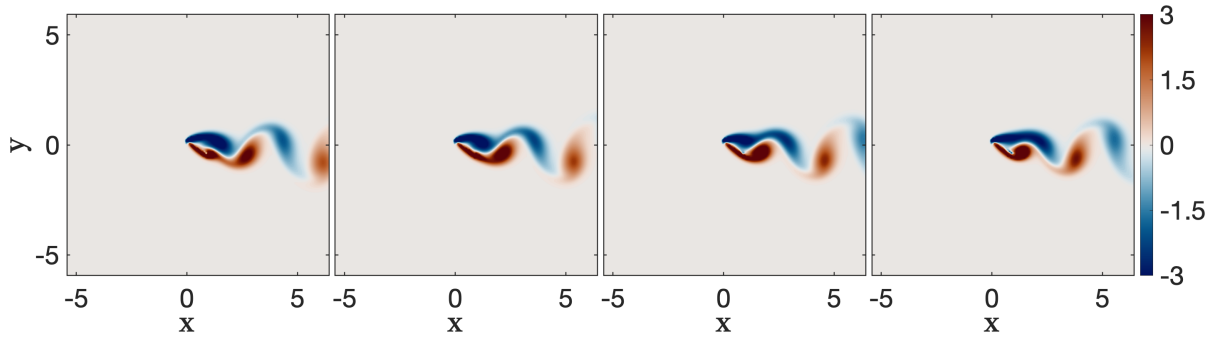

Fig. 1 Vorticity contours of flow past a flat plate at an angle of attack of 35 degrees at four different time instances.

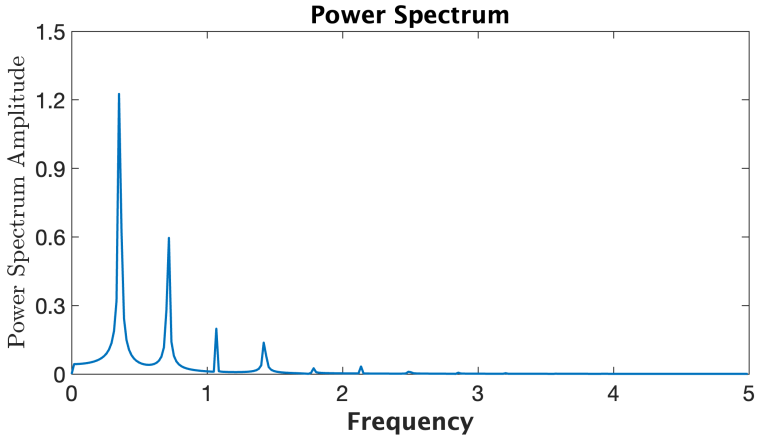

Fig. 2 Power spectrum of the flat plate vortex shedding, demonstrating the dominant Fourier modes

shedding, and the fourth a frequency of four times the vortex shedding. The odd modes (the first and third mode shown) are observed to be fairly top-down symmetric, with a maximum value near the center of the wake and a fairly vertical orientation of the modes. The even modes (the second and fourth modes shown) are observed to be fairly top-down antisymmetric, with a zero crossing near the center of the wake and oppositely signed structures above and below. There is only one dynamic time scale in the original data: the flow is laminar with a perfectly periodic limit cycle. Upon examining the Fourier modes, three key questions arise: Why do we need a cascade of Fourier modes to represent such a simple flow? Why do even Fourier modes have up-down anti-symmetry but not odd modes? Are the higher modes approximately harmonics along the x direction as well as time, and if so, why do they have that structure?

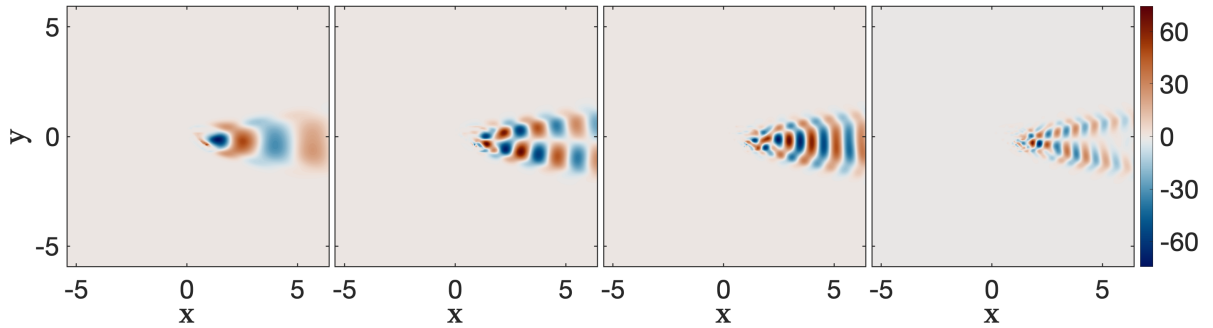

Fig. 3 The dominant Fourier modes of the flate plate vortex shedding

We suggest that skewness is important to answering these questions, and so turn now to the skewness distribution of this simple flow. To analyze the skewness of the flow, we compute the skewness of the vorticity field data at a particular (x, y) location in the flow field. In Figure 4a, we highlight a range of locations where skewness is evaluated: three different x locations are chosen, and the value of skewness throughout the wake is calculated. For reference, in the background of Figure 4a, an instantaneous snapshot of the wake is provided, but note that skewness is a statistical quantity calculated across all available time snapshots in the limit cycle of this system. In Figure 4b, the skewness values computed from the locations marked in Figure 4a are shown. Each streamwise position has a distinct color, and the skewness values are plotted against the y-coordinate. We see in Figure 4b that at a given streamwise position, the skewness varies from approximately 1 to approximately -1 as one moves from below the center of the wake to above the center of the wake. This skewness distribution is observed to be essentially constant in the streamwise direction, as can be seen by the collapse of the skewness distribution across the multiple colored markers. The vorticity field has this skewness because negative vortices are consistently shed from the leading edge on the top half of the wake, while positive vortices are consistently shed from the trailing edge on the bottom half of the wake. As these vortices convect downstream, there is a persistent and coherent up-down asymmetry in the flow dynamics. This leads to consistently larger negative excursions than positive excursions in the upper half of the wake, leading to negative skewness for the top half of the wake and the opposite for the bottom half of the wake. The skewness is not exactly symmetric up-down due to the angle of attack of the plate that generates a different strength of leading edge versus trailing edge vortices; for flow past a circular cylinder, for example, we would expect a perfectly symmetric skewness variation with y.

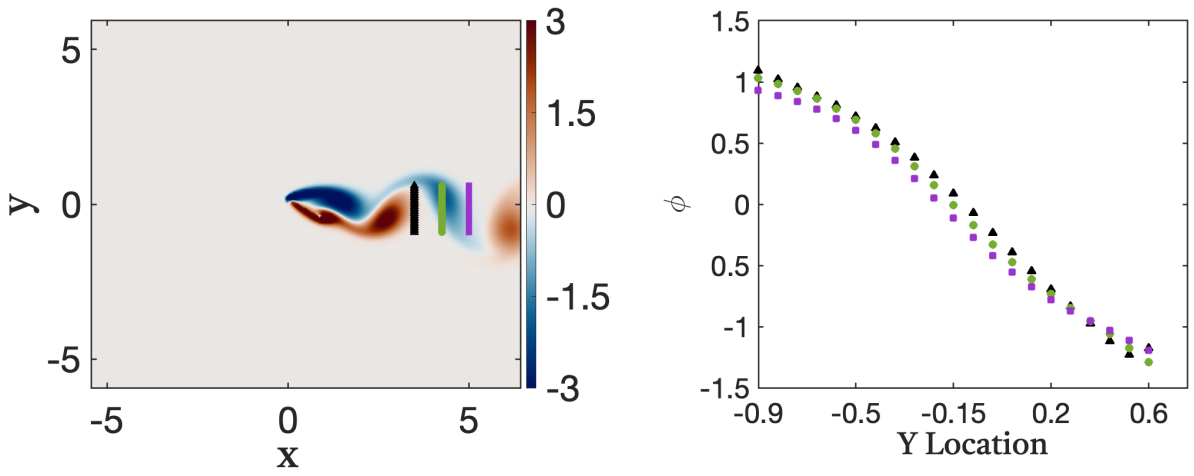

(a) **(b)**

Fig. 4 (a) Three streamwise locations, x, and multiple vertical locations, y, are highlighted in black, green, and magenta lines, indicating where skewness was calculated for (b). In (a), vorticity at a single time instance is plotted in the background for reference, but skewness is calculated across all time instances in the limit cycle. In (b), the skewness of the vorticity field is plotted against the variation in y for each of the streamwise locations, which are denoted with the same colors used in (a).

In the ensuing analysis, we seek to demonstrate that the existence of a cascade of Fourier modes, their up-down (a)symmetry and the streamwise harmonics observed in Figure 3 for the wake flow are a direct function of the skewness of the wake shown in Figure 4. To clarify these relationships, we turn now to a model problem, and will then finally relate our findings back to the flat plate vortex shedding problem.

IV. Mathematical relationship between skewness and Fourier modes

We employ a model problem depicting a continuous-time deterministic signal characterized by a harmonic series, augmented by a noise term,

$$s(t) = \sum_{r=1}^{N} \alpha_r \cos(r\omega_0 t + \gamma_r) + \sum_{p=1}^{M} \kappa_p \cos(\omega_p t). \tag{2}$$

Here α_r is the amplitude of each harmonic Fourier mode, with N total harmonics considered. The fundamental frequency is provided as ω_0 and the phase of each harmonic is given as γ_r. The noise is assumed to be dynamically distinct from the fundamental frequency, ω_0, such that $\omega_p \neq b\omega_0$, where b is any real number and no two ω_ps are harmonics of each other. We define the coefficient vector θ as

$$\theta = [\alpha_1, \alpha_2 ... \alpha_N, \gamma_1, \gamma_2, ... \gamma_N, \kappa_1, \kappa_2, \kappa_3, ..., \kappa_M]^T, \tag{3}$$

such that the signal can now be considered a function of both time and the coefficient vector: $s = s(\theta, t)$.

The skewness, ϕ, of the signal $s(\theta, t)$ is expressed mathematically as the third central moment divided by the cube of the standard deviation of the signal,

$$\phi_{(s(\theta,t))} = \frac{E\{s^3(\theta,t)\}}{(E\{s^2(\theta,t)\})^{3/2}}. \tag{4}$$

For the sake of clarity, we focus first on the numerator and define the numerator of the skewness as $\mathcal{N} = E\{s^3(\theta,t)\}$. In seeking an expression for the skewness, ϕ, of the deterministic and periodic signal $s(\theta,t)$, we first determine the expectation, which for a deterministic periodic signal is equivalent to the time average,

$$\mathcal{N} = \frac{\omega_0}{2\pi} \int_0^{2\pi/\omega_0} s^3(\theta,t) dt. \tag{5}$$

Upon substituting the specific form of $s(\theta,t)$ into the expression for $\mathcal{N}$, the numerator can be decomposed into several parts, each reflecting different interactions of the sinusoidal components $\mathcal{N} = \mathcal{N}_1 + \mathcal{N}_2 + \mathcal{N}_3 + \mathcal{N}_4$, where

$$\mathcal{N}_1 = \frac{\omega_0}{2\pi} \int_0^{2\pi/\omega_0} \left(\sum_{r=1}^{N} \alpha_r^3 \cos^3(r\omega_0 t + \gamma_r) + \sum_{p=1}^{M} \kappa_p^3 \cos^3(\omega_p t) \right) dt,$$

$$\mathcal{N}_2 = \frac{\omega_0}{2\pi} \int_0^{2\pi/\omega_0} \left(3 \sum_{r=1}^{N} \alpha_r^2 \cos^2(r\omega_0 t + \gamma_r) \left(\sum_{i=1, i\neq r}^{N} \alpha_i \cos(i\omega_0 t + \gamma_i) + \sum_{p=1}^{M} \kappa_p \cos(\omega_p t) \right) \right) dt,$$

$$\mathcal{N}_3 = \frac{\omega_0}{2\pi} \int_0^{2\pi/\omega_0} \left(3 \sum_{p=1}^{M} \kappa_p^2 \cos^2(\omega_p t) \left(\sum_{r=1}^{N} \alpha_r \cos(r\omega_0 t + \gamma_r) + \sum_{q=1, q\neq p}^{M} \kappa_q \cos(\omega_q t) \right) \right) dt,$$

$$\mathcal{N}_4 = \frac{\omega_0}{2\pi} \int_0^{2\pi/\omega_0} (A)$$

$$A = \left(\sum_{r=1}^{N} \sum_{i=1, i\neq r}^{N} \alpha_r \cos(r\omega_0 t + \gamma_r) \alpha_i \cos(i\omega_0 t + \gamma_i) \left(\sum_{j=1, j\neq r, j\neq i}^{N} \alpha_j \cos(j\omega_0 t + \gamma_j) + \sum_{p=1}^{M} \kappa_p \cos(\omega_p t) \right) \right.$$
$$\left. + \sum_{p=1}^{M} \sum_{q=1, q\neq p}^{M} \kappa_p \cos(\omega_p t) \kappa_q \cos(\omega_q t) \left(\sum_{r=1}^{N} \alpha_r \cos(r\omega_0 t + \gamma_r) + \sum_{s=1, s\neq p, s\neq q}^{M} \kappa_s \cos(\omega_s t) \right) \right) dt.$$

These four parts of the numerator can be categorized into three classes [3]. The mathematical expressions describe specific conditions under which the integral terms in the equations evaluate to non-zero values due to frequency matching or mismatching. $\mathcal{N}_1$ represents a class of integrals with purely cubed sinusoids. By definition, we can say that

$$\mathcal{N}_1 = 0. \tag{6}$$

Parts $\mathcal{N}_2$ and $\mathcal{N}_3$ represent parts that contain a squared sinusoid multiplied with another sinusoid of different frequency. These integrals are only nonzero for specific values of r and i. In cases where $i = 2r$, parts of $\mathcal{N}_2$ are nonzero [3]. Consequently, $\mathcal{N}_2$ can be expressed as

$$\mathcal{N}_2 = \begin{cases} \sum_{r=1}^{N} \sum_{i\neq r}^{N} \alpha_r^2 \alpha_i \mathcal{F}(\gamma_r, \gamma_i), & \text{if } i = 2r \\ 0, & \text{otherwise} , \end{cases} \tag{7}$$

with

$$\mathcal{F}(\gamma_r, \gamma_{i=2r}) = \left(-\frac{3}{4}\cos(\gamma_i) + \frac{3}{2}\cos^2(\gamma_r)\cos(\gamma_i) + \frac{3}{2}\cos(\gamma_r)\sin(\gamma_r)\sin(\gamma_i) \right). \tag{8}$$

Note that $\mathcal{N}_3$ is always zero, as are the terms that involve the noise terms in $\mathcal{N}_2$ because they cannot satisfy a duplicative relationship between frequencies highlighted in equation 7.

Finally, $\mathcal{N}_4$ is nonzero only when $r = i \pm j$, or equivalently when the three frequencies are triadically consistent [3]. $\mathcal{N}_4$ can be expressed as:

$$\mathcal{N}_4 = \begin{cases} \sum_{r=1}^{N} \sum_{i=1, i\neq r}^{N} \sum_{j=1, j\neq i, j\neq r}^{N} \alpha_r \alpha_i \alpha_j \mathcal{G}(\gamma_r, \gamma_i, \gamma_j), & \text{if } j = r \pm i \\ 0, & \text{otherwise} \end{cases}, \tag{9}$$

with

$$\mathcal{G}(\gamma_r, \gamma_i, \gamma_j) = -\frac{3}{2}\sin(\gamma_r)\sin(\gamma_i)\cos(\gamma_j) + \frac{3}{2}\sin(\gamma_r)\cos(\gamma_i)\sin(\gamma_j) \tag{10}$$

$$+ \frac{3}{2}\cos(\gamma_r)\sin(\gamma_i)\sin(\gamma_j) + \frac{3}{2}\cos(\gamma_r)\cos(\gamma_i)\cos(\gamma_j). \tag{11}$$

The function $\mathcal{G}(\gamma_r, \gamma_i, \gamma_j)$ describes the phase relationships between the three interacting waves, influencing the magnitude and sign of the interaction based on how the phases align. Note that again, all terms associated with the noise terms yield results of zero in $\mathcal{N}_4$.

The total skewness of the signal s can therefore be written as

$$\phi(s) = \frac{\begin{cases} \sum_{r=1}^{N} \sum_{i=1, i\neq r}^{N} \alpha_r^2 \alpha_i \mathcal{F}(\gamma_r, \gamma_i), & \text{if } i = 2r \\ 0, & \text{otherwise} \end{cases}}{\left(\frac{1}{2}\sum_{r=1}^{N}(\alpha_r^2) + \frac{1}{2}\sum_{p=1}^{M}\kappa_p^2 \right)^{\frac{3}{2}}} +$$

$$+ \frac{\begin{cases} \sum_{r=1}^{N} \sum_{i=1, i\neq r}^{N} \sum_{j=1, j\neq i, j\neq r}^{N} \alpha_r \alpha_i \alpha_j \mathcal{G}(\gamma_r, \gamma_i, \gamma_j), & \text{if } j = r \pm i \\ 0, & \text{otherwise} \end{cases}}{\left(\frac{1}{2}\sum_{r=1}^{N}(\alpha_r^2) + \frac{1}{2}\sum_{p=1}^{M}\kappa_p^2 \right)^{\frac{3}{2}}}$$

$$\phi(s) = \frac{\mathcal{N}_2 + \mathcal{N}_4}{\left(\frac{1}{2}\sum_{r=1}^{N}(\alpha_r^2) + \frac{1}{2}\sum_{p=1}^{M}\kappa_p^2 \right)^{\frac{3}{2}}} \tag{12}$$

We can learn a lot from this re-written form of skewness. First, note that, for the special case of

$$s_0(\theta, t) = \alpha_0 \cos\left(\omega_0 t + \gamma_0\right), \tag{13}$$

in which the signal can be represented by a single sinusoid, then the skewness of this special type of signal can be written using only the part of the numerator $\mathcal{N}_1$, as there is only one frequency. We can therefore immediately say that the skewness of such a signal is zero from equation 6. We can therefore see that, if a signal $s(\theta, t)$ has non-zero skewness, then it must be represented by more than one mode. Regardless of the level of periodicity of a signal, if it has non-zero skewness, multiple Fourier modes will be needed to represent that signal.

In order to represent a skewed signal, we specifically need modes that have relationships between their frequencies: either $\omega_i = 2\omega_r$ or $\omega_j = \omega_r \pm \omega_i$. To represent a skewed signal, the Fourier transform of that signal must include harmonic or triadically consistent modes. The inspection of this model provides clarity on why harmonics appear in the Fourier transforms of simple fluid dynamics problems. For fluid dynamics systems that have non-zero skewness, including the laminar vortex shedding problem discussed in section III, the Fourier transform must include multiple harmonic or triadically consistent modes to reconstruct the flow field.

Next, we ask why the Fourier modes of the vorticity field that we observe in figure 3 have particular types of symmetry. We note that the first and third modes are approximately symmetric top-down about the center of the wake (along $y \approx 0$), while the second and fourth mode are approximately antisymmetric top-down about the center of the wake (along $y \approx 0$). We will argue that the change in sign of skewness as one passes through the wake vertically requires

that the even modes exhibit a phase change of π as one moves vertically through the wake, which is consistent with the antisymmetric shape of the even modes observed.

Returning to the 1D model system, the sign of the skewness is controlled by the functions $\mathcal{F}$ and $\mathcal{G}$ in equation 12, as the amplitudes α_r are defined to be positive. The phase of the Fourier modes will be different at different points in space, and it is that phase variation that must represent the positive and negative sign of the skewness at particular locations. We take three approaches here to give the reader intuition for how $\mathcal{F}$ is related to the observed structure of the first and second Fourier modes. First, we plot the variation of $\mathcal{F}$ with the phases of two modes, γ_r and γ_i, in Figure 5. Second, we consider two model signals that have a simple phase difference in their relationship and inspect their differing skewnesses. Finally, we evaluate the phases of the fourier modes of the flow problem of flow past the flat plate. In each case, we identify that a specific phase change between the first and second fourier mode is consistent with a change in the sign of skewness.

The function $\mathcal{F}$ from equation 8 dictates the sign variation of the N_2 part of the skewness signal, and $\mathcal{F}$ is a function of the phases of the Fourier modes. To better understand the variation of $\mathcal{F}$, we consider the first two Fourier modes, which satisfy the relation $i = 2r$. Figure 5 illustrates the variation of $\mathcal{F}$ by varying the phases of two modes with the relation $i = 2r$, γ_r and γ_i. Both γ_r and γ_i are ranged between -2π and 2π. When γ_r is kept constant, a π change in γ_i is required to change the sign of $\mathcal{F}$. Conversely, when γ_i is fixed, a $\frac{\pi}{2}$ change in γ_r is needed for $\mathcal{F}$ to change its sign.

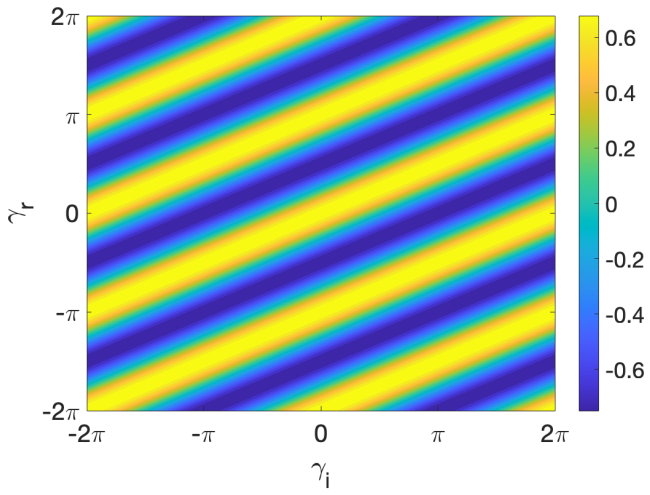

Fig. 5 Variation of $\mathcal{F}$ with γ_r and γ_i for $i = 2r$.

As one moves through the wake of the flat plate vertically, skewness changes sign (Figure 4b) and we argue that in the fourier modes this is represented with the first mode having an approximately constant phase (equivalent to γ_r constant), while the second mode has the needed π phase change. To show this, the vorticity signal in time was extracted from each point in the domain and an independent fourier transform was performed for each location. From the phases of these fourier modes, $\mathcal{F}$ for modes 1 and 2 and $\mathcal{G}$ for modes 1, 2, and 3 were computed at each spatial location and plotted in Figure 6. After a complex structure near the flat plate, the functions settle in the wake with a roughly antisymmetric up-down symmetry and slow variation with x, as is expected due to the form of skewness in the wake. To generate a sign change in skewness and in $\mathcal{F}$, Figure 5 suggests that γ_r can remain constant, while γ_i changes by π. Three sets of points were chosen in the wake that have equal and opposite skewness and are vertically aligned, highlighted in Figure 7(a). The phase of the first four fourier modes were identified at each of the points, and the differences in their phases was compared within each pair. Figure 7b plots the phase difference within the pairs of spatial points that had equal and opposite skewness. The phase differences among corresponding odd harmonic modes were observed to be stay near 0, while the phase differences for corresponding even harmonics approached 180 degrees. This is consistent with expectations from Figure 5. This observation implies a synchronized behavior among odd harmonics and an anti-phase relationship among even harmonics for points with opposite skewness. The out-of-phase characteristic in even harmonics is consistent across all examined pairs of spatial points characterized by opposing skewness values.

We can relate these observations about the sign change in the even temporal harmonics to the structure of the spatial

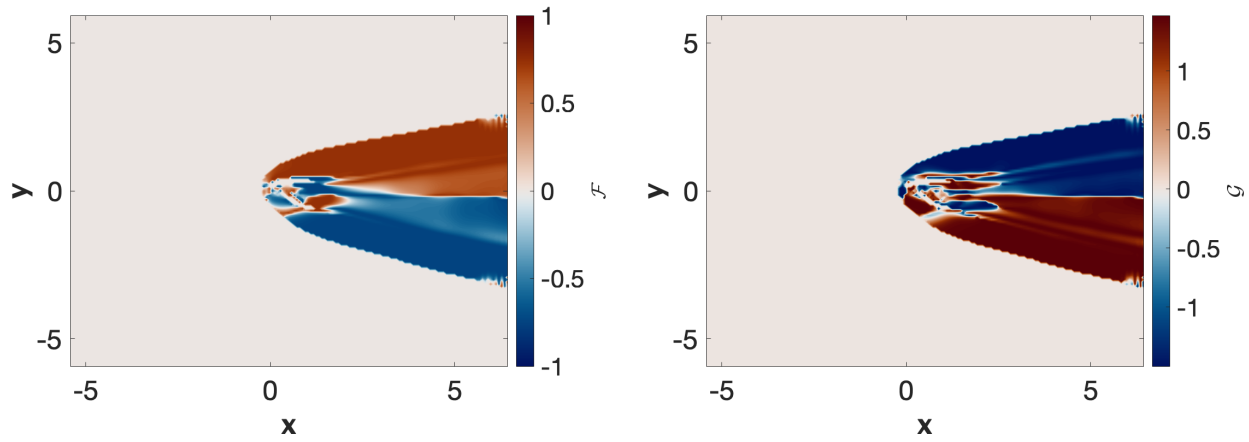

(a) (b)

Fig. 6 The contour plot of $\mathcal{F}$ and $\mathcal{G}$ across the entire wake of the flat plate

fourier modes in Figure 3 by first understanding how we interpret the spatial variation of the mode in terms of the mode's phase. A mode with a consistent color in a region of space we interpret as having little to no phase change between those points, while a mode with a change from red to blue in space indicates a phase change of π between those points. As we move vertically down in the wake in Figure 3, the first mode shows little change in phase, while the second mode shows a π change in phase. We can now understand from Figure 5 that this symmetric (no phase change) odd mode and antisymmetric (π phase change) even mode structure will succeed in representing the change in sign of skewness across the wake vertically. Note that this analysis focuses on $\mathcal{F}$, but similar analysis can be undertaken for $\mathcal{G}$ and for the subsequent higher modes. Future work will attempt to explain the original phase organization of mode 1; once the phase organization of the first mode is identified, all other modes' vertical phase organizations then follow from the requirement that the modes collectively represent the skewness field.

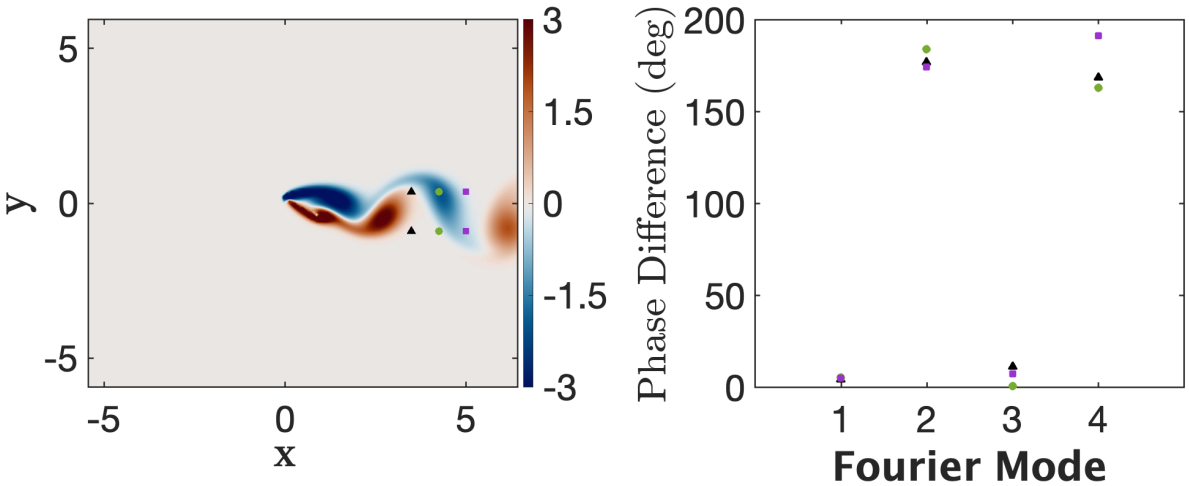

(a) (b)

Fig. 7 (a) Pairs of points with equal and opposite skewness at three different streamwise positions. Fourier modes are computed from the time series at each point in (a). The phase difference between the pair of points with the same marker in (a) for the 4 dominant Fourier modes are shown in (b).

To demonstrate the relationship between fourier mode phase and the overall skewness in a simple and direct manner,

we consider two simple signals,

$$s_1(t) = \alpha_1 \cos(\omega_0 t) + \alpha_2 \cos(2\omega_0 t) + \alpha_3 \cos(3\omega_0 t) + \alpha_4 \cos(4\omega_0 t) + \alpha_5 \cos(5\omega_0 t) \tag{14}$$

and

$$s_2(t) = \alpha_1 \cos(\omega_0 t) + \alpha_2 \cos(2\omega_0 t + \pi) + \alpha_3 \cos(3\omega_0 t) + \alpha_4 \cos(4\omega_0 t + \pi) + \alpha_5 \cos(5\omega_0 t). \tag{15}$$

The two model signals are constructed using the same five frequencies with the same amplitudes for each harmonic. The only difference between the two signals is that in $s_1(t)$, all harmonics have the same phase, while for $s_2(t)$, even harmonics are shifted by a phase shift of π.

Using the final form of skewness(ϕ) in (12), the skewness for both the signals becomes

$$\phi_{s_1} = \frac{\frac{3}{4}\alpha_1^2\alpha_2 + \frac{3}{4}\alpha_2^2\alpha_4 + \frac{3}{2}\alpha_1\alpha_2\alpha_3 + \frac{3}{2}\alpha_1\alpha_3\alpha_4 + \frac{3}{2}\alpha_1\alpha_4\alpha_5 + \frac{3}{2}\alpha_2\alpha_3\alpha_5}{(\frac{1}{2}\sum_{r=1}^{5}(\alpha_r^2))}, \tag{16}$$

$$\phi_{s_2} = \frac{-\frac{3}{4}\alpha_1^2\alpha_2 - \frac{3}{4}\alpha_2^2\alpha_4 - \frac{3}{2}\alpha_1\alpha_2\alpha_3 - \frac{3}{2}\alpha_1\alpha_3\alpha_4 - \frac{3}{2}\alpha_1\alpha_4\alpha_5 - \frac{3}{2}\alpha_2\alpha_3\alpha_5}{(\frac{1}{2}\sum_{r=1}^{5}(\alpha_r^2))}. \tag{17}$$

And so $\phi_{s_1} = -\phi_{s_2}$. The two signals have skewness equal in magnitude and opposite in sign with a phase shift of π in the even harmonics' phase.

Having connected the skewness of the flow to the need for temporal harmonics as well as the vertical symmetric and antisymmetric structure of odd and even modes, we end by exploring whether we can connect our observations about skewness to the observation of higher spatial wavenumbers in x for the higher modes. If so, one may be able to predict much of the structure of the harmonic fourier modes only from the skewness field. We approach the question of the spatial variation of the modes in x from a phase perspective, asking how quickly the phase of the modes must change in x, which provides insight into the approximate spatial frequency of the mode.

For the wake problem, we identified in Figure 4b that the skewness of the flow does not change substantially in x and in Figure 6 that $\mathcal{F}$ and $\mathcal{G}$ change slowly with x. We plot the variation of $\mathcal{F}$ with x for modes 1 for two cases: $(r = 1, i = 2)$ and $(r = 2, i = 4)$ in Figure 8a(b,c). The phases are evaluated at the points in Figure 8a(a), along a line of constant y in the wake (we acknowledge that the wake is also expanding, so there likely is a different curve through space that would better line up with a constant $\mathcal{F}$). We observe that $\mathcal{F}$ remains almost constant in the developed wake region.

Knowing that $\mathcal{F}$ is relatively constant with x, we turn to Figure 5 to understand the relationship between $\mathcal{F}$ and the phases of the fourier modes along x. In Figure 5, we observe that lines of constant $\mathcal{F}$ have a slope of two. To stay on lines of constant $\mathcal{F}$, γ_i must change twice as quickly as γ_r. This rate of phase change can be expressed in terms of frequency. If mode 1 changes by $\pi/2$ over some distance, mode 2 must change by π, indicating that mode 2 has a spatial frequency twice that of mode 1. This explains the spatial harmonics observed as we move in the streamwise direction; the doubling of the spatial frequency alongside the doubling of the temporal frequency is necessary to represent a flow along directions of the flow with no skewness variation.

V. Discussion

From these analyses, we argue that many features of fourier modes can be deduced apriori from inspection of the skewness distribution of this flow. Because there is non-zero skewness, we immediately can predict that we will need to use multiple harmonics to reproduce this flow with a fourier series, based on equation 6. From the spatial distribution of skewness, which features a change of sign as one moves vertically through the wake, we can predict a phase variation in the even Fourier harmonics, yielding a symmetric spatial structure about the center of the wake in the odd harmonics and an antisymmetric spatial structure about the center of the wake in the even harmonics. From the constancy of the skewness of in the streamwise direction, we can say that the fourier modes with harmonic relationships in time will have an equivalent spatial harmonic structure. The piece that we cannot determine apriori from this analysis is the fundamental frequency of the first mode and its spatial wavenumber; the frequency and wavenumber are known to be related to the speed of the flow and the size of the obstacle through the Strouhal number [8]. With that physical insight in hand, alongside this analysis, we suggest that the fourier modes could be predicted without their calculation.

We also highlight that the higher harmonics are not truly separate scales of dynamic relevance, but instead are 'corrections' to the first mode that build the appropriate skewness and asymmetry into the final reconstruction. In future work, we will explore whether there are alternative basis functions that can more succinctly represent skewed flows by including skewed behavior in the basis vectors.

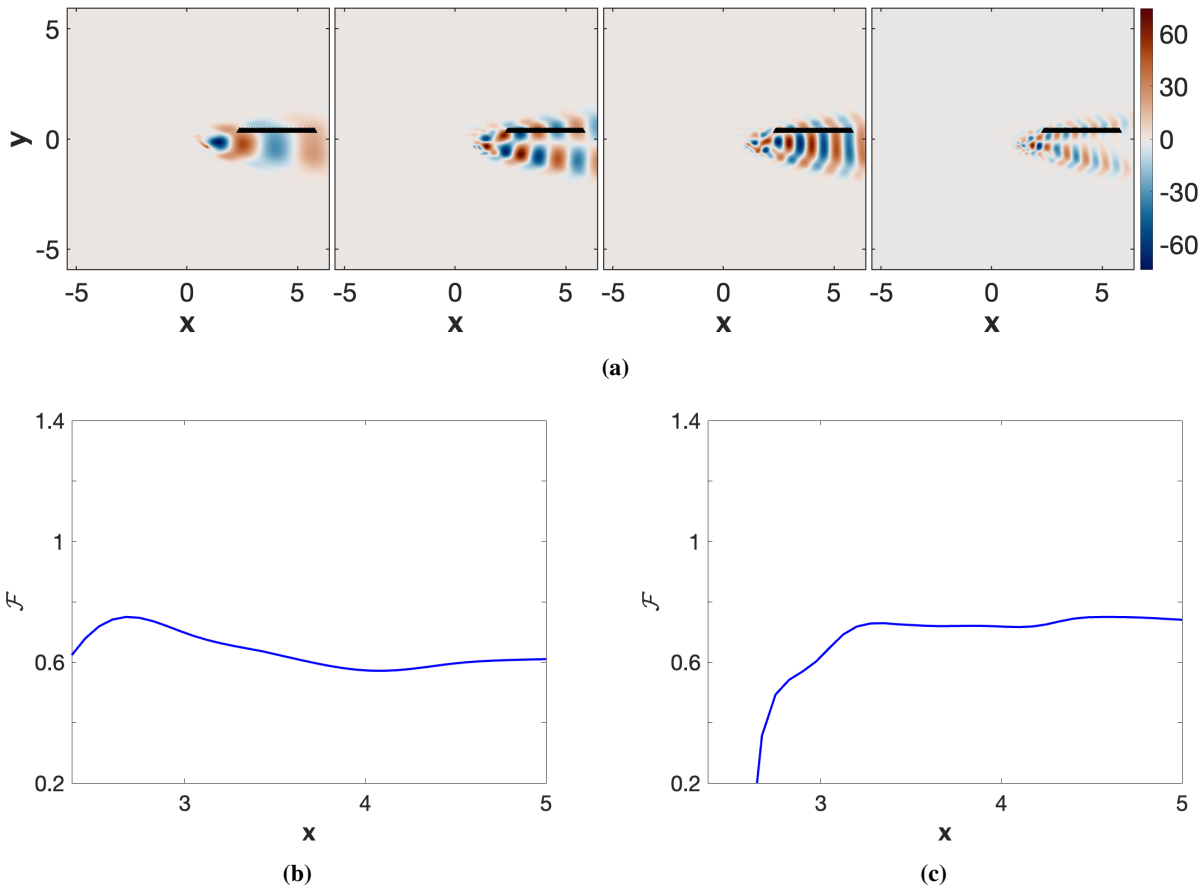

Fig. 8 (a) Locations in the wake at constant y for which the variation of $\mathcal{F}$ with x was calculated for two cases. (a) For Mode 1 and Mode 2, where r = 1 and i = 2. (b) For Mode 2 and Mode 4, where r = 2 and i = 4

VI. Conclusions

Our manuscript began with performing a Fast Fourier Transform (FFT) on the vorticity data of the flat plate vortex shedding. This analysis revealed four distinct peaks, with each subsequent peak representing consecutive harmonics of the fundamental frequency. Additionally, the spatial Fourier modes associated with these specific frequencies were presented. The skewness of the wake of a flat plate at an angle of attack was studied as a function of space, and the skewness at different spatial locations in the wake exhibited consistency in the streamwise direction and a meaningful distribution in the vertical direction, corresponding to the sign of shed vorticity. An analysis of the mathematical form of skewness for a general signal revealed its relationships to the harmonics of the signal. It was observed that only modes with specific relationships can represent the overall skewness of the signal. From analysis of this relationship, we identified that a single Fourier mode is not able to represent a skewed signal, and that harmonics and triadically consistent modes are required to represent a skewed signal. The implications of the skewness / Fourier mode relationship on the spatial structure of Fourier modes was also considered. By examining the variation of $\mathcal{F}$ with the phases of the first and second Fourier modes, analyzing model signals with simple phase differences, and evaluating the phases in the flow past a flat plate, we identified a consistent phase change linked to skewness sign changes. Spatial points with opposite skewness values exhibited in-phase behavior for odd harmonic Fourier modes and out-of-phase behavior for even harmonic modes. The two-dimensional Fourier modes demonstrated up-down symmetry in odd harmonic modes and up-down anti-symmetry in even harmonic modes, highlighting the physical interpretation of Fourier modes in skewed flows. Modes that were harmonics in time were found to also be harmonics in their spatial wavenumber along curves of constant skewness, which in this flow was approximately horizontal lines.Cumulatively, these findings shed light on the intimate connection between the harmonics in Fourier modes and the underlying skewness of the signal and provide insight into why such a simple flow requires a cascade of harmonics to be appropriately represented with a

Fourier transform. Future work is suggested to generalize some of the analysis shown here to higher modes and to explain the structure of the first mode. We also suggest that the skewness field and simple physical scaling laws may be sufficient to predict the Fourier modes without their computation, and the demonstration of such predictive capability is left for future work.

Acknowledgments

We gratefully acknowledge the support of the National Science Foundation through Grant No. 2118209. We also acknowledge useful discussions with Akhileshwar Borra, Zoey Flynn, and Andres Goza.

References

[1] Sirovich, L., and Knight, B. W., "The Eigenfunction Problem in Higher Dimensions: Asymptotic Theory," *Proceedings of the National Academy of Sciences of the United States of America*, Vol. 82, No. 24, 1985, pp. 8275–8278. URL http://www.jstor.org/stable/26569.

[2] Foias, C., Manley, O., and Sirovich, L., "Empirical and Stokes eigenfunctions and the far-dissipative turbulent spectrum," *Physics of Fluids A: Fluid Dynamics*, Vol. 2, No. 3, 1990, pp. 464–467. https://doi.org/10.1063/1.857744, URL https://doi.org/10.1063/1.857744.

[3] Ovacıklı, A. K., Pääjärvi, P., LeBlanc, J. P., and Carlson, J. E., "Uncovering harmonic content via skewness maximization - a Fourier analysis," 2014, pp. 481–485.

[4] Schlatter, P., and Örlü, R., "Quantifying the interaction between large and small scales in wall-bounded turbulent flows: A note of caution," *Physics of Fluids*, Vol. 22, No. 5, 2010, p. 051704. https://doi.org/10.1063/1.3432488, URL https://doi.org/10.1063/1.3432488.

[5] Mathis, R., Marusic, I., Hutchins, N., and Sreenivasan, K. R., "The relationship between the velocity skewness and the amplitude modulation of the small scale by the large scale in turbulent boundary layers," *Physics of Fluids*, Vol. 23, No. 12, 2011, p. 121702. https://doi.org/10.1063/1.3671738, URL https://doi.org/10.1063/1.3671738.

[6] Duvvuri, S., and McKeon, B. J., "Triadic scale interactions in a turbulent boundary layer," *Journal of Fluid Mechanics*, Vol. 767, 2015, p. R4. https://doi.org/10.1017/jfm.2015.79.

[7] Goza, A., and Colonius, T., "A strongly-coupled immersed-boundary formulation for thin elastic structures," *Journal of Computational Physics*, Vol. 336, 2017, pp. 401–411. https://doi.org/https://doi.org/10.1016/j.jcp.2017.02.027, URL https://www.sciencedirect.com/science/article/pii/S0021999117301201.

[8] Roshko, A., "On the development of turbulent wakes from vortex streets," 1953. URL https://api.semanticscholar.org/CorpusID:15843746.